Geotechnical Aspects of Underground Construction in Soft Ground, Kusakabe, Fujita & Miyazaki (eds)


# Stress paths around a 3-D numerically simulated NATM tunnel in stiff clay

D.K.W.Tang, K.M.Lee & C.W.W.Ng
*Civil Engineering Department, Hong Kong University of Science and Technology, People's Republic of China*

ABSTRACT: The use of New Austrian Tunnelling Method (NATM) in soft ground has been increased worldwide in recent years because of its great flexibility. Tunnel excavation adopting the NATM is usually divided into sub-sections which are to be excavated under sequential steps. The excavation of each sub-section is then followed by the application of temporary reinforcements. Different unsupported span lengths in the longitudinal direction at each step has considerable effects on stress redistribution in the ground, soil deformations as well as stress induced in tunnel supporting systems. In this study, Type 2 construction sequence in the Heathrow Express Trial Tunnel is simulated by 3D elasto-plastic coupled-consolidation finite element analyses. Ground deformations, stress changes and excess pore water pressure around the tunnel opening are predicted by the numerical analyses. Results are compared with those measured on site. Stress paths of those representative positions around the tunnel opening during the excavation are obtained and discussed.

## 1 INTRODUCTION

The New Austrian Tunnelling Method (NATM) is a technique in which ground exposed from excavation is temporarily supported by shotcrete as lining. The main advantage of NATM over conventional techniques is its outstanding flexibility. Many different support techniques can be adopted to deal with various ground conditions. In additions, it can provide immediate and flexible support of freshly excavated ground, allow non-circular tunnels, easier construction of large complex sections and the potential for cost saving is very high. Many successful cases of tunnelling using the NATM have been reported recently (Murphy 1993, McWilliam 1991).

Ground movements as well as stress distribution due to tunnelling is three dimensional in nature (Peck 1969, Ranken and Ghaboussi 1975). The face movement of ground can become large if a considerable degree of soil yields into the face. Three-dimensional numerical analyses for tunnelling problems have been conducted by a number of researchers (Swoboda et. al 1989, Lee and Rowe 1990, Lee and Rowe 1991, Chen and Bauldauf 1994, Desari, et. al. 1996). Swoboda et. al. (1989) used a rheological model to analysed a NATM tunnel in rocks in order to understand the time-dependent interaction between shotcrete and ground deformations. Desari et. al. (1996) reproduced the Type 2 construction of the Heathrow Express Trial Tunnel in both 2D and 3D. The lining was assumed either wished-in-place or introduced after the excavation of each panel and the construction sequence of lining was investigated.

The aim of this paper is to simulate the Type 2 construction (to be defined in the following section) of the Heathrow Express Trial tunnel in three dimensions. Different lengths of the unsupported spans were modelled so as to try to fit those measured. Stress paths around the tunnel opening during the excavation are examined.

## 2 HEATHROW TRIAL TUNNEL

The Heathrow Express Trial Tunnel was the first tunnel excavated by the New Austrian Tunnelling Method (NATM) in the London Clay. The tunnel is located on a section of the proposed tunnel alignment running from the Central Terminal Area to the Terminal 4 station.

The tunnel section is of oval shape that the height of the tunnel is about 8m while the width of the section is about 9m. The tunnel has a face area of about 59m$^2$ and an axial depth below the ground surface of approximately 20m. At the trial tunnel, 3 different kinds of construction sequences were evaluated to examine the performance and suitability. The length of the tunnel is 100m which is divided into 3 different excavation sequences each over a length of about 35m. The three trial designs were based on excavation sequences successfully used elsewhere in Europe. Type 1 construction sequence was the most conservative and consisted of two side headings followed by the removal of the central core of the tunnel. Type 2 was to excavate one side of the tunnel and then enlarge it to its full size. The third type was a top heading and bench sequence with the bottom of the shotcrete arch of the heading supported on inverted shotcrete arches (Deane and Bassett 1995, New and Bowers 1994). Field observation indicated that the Type 2 construction sequence gave the best performance in terms of settlement among the three types of construction, thus, the Type 2 excavation scheme is investigate in this study. The Type 2 construction is distinctively asymmetric, the left drift of 29.8m$^2$ are being completed prior to the right drift (28.8m$^2$). Lining consisted of a 250mm shotcrete shell with a single layer of steel mesh and lattice girders at 1m centres along the tunnel were used. Twelve days were taken for excavation of the left drift and another twelve days for the remaining part of the tunnel.

For the Type 2 construction sequence, the maximum ground surface settlement measured for the left drift and on the completion of the excavation was 14.5mm and 26.8mm, respectively, while the volume loss was determined as 1.24% and 1.05%, respectively. The standard deviation, *i*, which provides a means of defining the trough width, was 9m on the completion of the excavation.

## 3 3D MODELLING OF NATM

### 3.1 *Geometry and sequence of excavation*

The analyses are performed with the finite element program, ABAQUS (Hibbitt, Karlsson & Sorensen, Inc 1997). Figure 1 shows the tunnel geometry and the modelled soil profile. The excavation of the oval tunnel of about 8.6m in diameter in London Clay was modelled. The excavation rate is assumed to be about 2.5m per day for either the left or the right drift. After the excavation step, lining is applied to the excavated surface in sequential steps, leaving a certain unsupported span constantly. The sequence of the excavation was modelled as:

1. excavate the left half of the tunnel;
2. shotcrete lining is installed on the exposed surface after the excavation by leaving a particular unsupported span behind the tunnel face (i.e. 5 m or 10 m);
3. after finishing the left drift, excavate the right half of the tunnel;
4. installation of the lining as in (2).

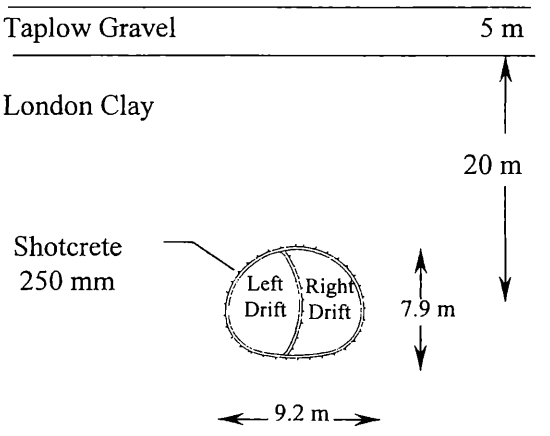


Figure 1. Tunnel geometry and the modelled soil profile.

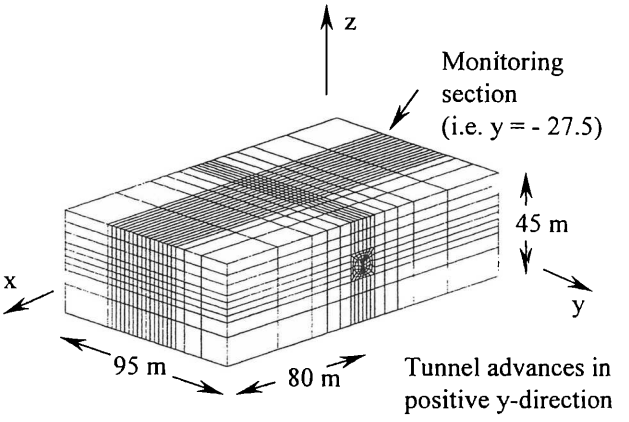


Figure 2. 3D Finite element mesh.

It should be noted that the excavation sequence in the numerical simulation has been simplified. The actual excavation section in the Trial Tunnel is subdivided into the top and bottom sections for both the left drift and the right drift.

### 3.2 *Finite element analysis*

In the analyses, 8-noded brick elements and 4-noded shell elements are used to model the soil and the shotcrete lining. Each corner node of 8-noded isoparametric elements has three degrees of freedom in displacement and one in pore pressure. The shell elements modelled the 250mm thick shotcrete lining, with a unit weight of 24kN/m$^3$. The Young's Modulus of shotcrete was taken as 30 x 10$^6$ kN/m$^3$, and the Poisson's Ratio was 0.3. Figure 2 shows the three-dimensional finite element mesh adopted in the study. The boundary conditions around the sides are retrained in one direction of movement which is normal to the corresponding side only. For the base of the mesh, movements in all the directions are restrained as well as the pore water pressure is fixed as the hydrostatic value.

The soil is assumed to have an elastic-perfectly plastic constitutive relationship that was defined by five cross-anisotropic elastic variable, $E_v$, $E_h$, $\nu_{vh}$, $\nu_{hh}$ and $G_{vh}$. The modified Drucker Prager failure criterion is adopted for the analyses.

The Taplow Gravel stratum located at the ground surface was modelled as being linear elastic with a modulus of 75 x 10$^3$ kN/m$^3$ and poisson ratio of 0.2. The London Clay was described by an anisotropic elastic-plastic model with soil parameters very similar to that determined for the London Clay at the New Queen Elizabeth II Conference Center excavation site (Burland and Kalra 1986). The gravel and the London clay were attributed with a coefficient of permeability of 1 x 10$^{-4}$ m/s and 1 x 10$^{-9}$ m/s, respectively. The initial stresses prescribed a hydrostatic pore water pressure profile from a water table located 5m below the ground surface. As the Coefficient of Earth Pressure at Rest, $K_o$, ranging from 1 to 2 was measured on site, a value of 1.5 is adopted in this study.

Excavation was modelled by removal of the solid elements within the tunnel boundary with the simulated rate of excavation of 2.5m per day for either the left or the right drift. Tunnel lining application is simulated by the reactivation of the lining (shell) element where they have been removed in the beginning. The elements are reactivated at their zero-stress state (also zero strain and plastic strain, etc.) in the configuration in which they lie at the start of the reactivation step. Since these elements are reactivated in a zero-stress state (i.e. with zero stress), they exert zero nodal forces on the rest of the model. This result allows reactivation to be done immediately, without an adverse effect on the smoothness of the solution.

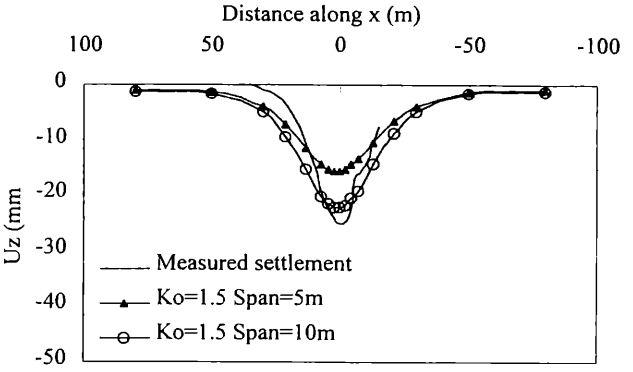


Figure 3. Transverse ground surface settlement on the completion of the excavation.

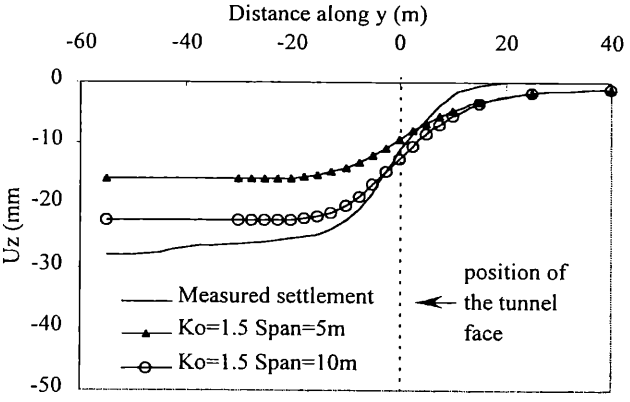


Figure 4. Longitudinal ground surface settlement along the centreline of the tunnel

## 4 RESULTS

### 4.1 *Surface Settlement*

In Figure 3, the predicted transverse ground surface settlement profiles with unsupported length of 5 m and 10 m are compared with the measured ground surface in the Heathrow Express Trial Tunnel. The measured ground surface settlement profiles are nonsymmetrical about the centreline of the tunnel due to the nonsymmetrical excavation sequence. The volume losses predicted from the analyses are 1.1% and 1.5% for the unsupported span length of 5 m and 10 m, respectively. This is consistent with the value determined at the site of 1.1%. Furthermore, the predicted shapes of the transverse ground settlement troughs are wider than the measured results.

Figure 4 show the longitudinal ground surface settlement along the centreline of the tunnel. The maximum settlement predicted from the analyses are 16 mm and 22 mm which underestimate the field measured value of 28 mm. In additions, the ground surface settlement occurred ahead of the tunnel face agrees with that measured on site.

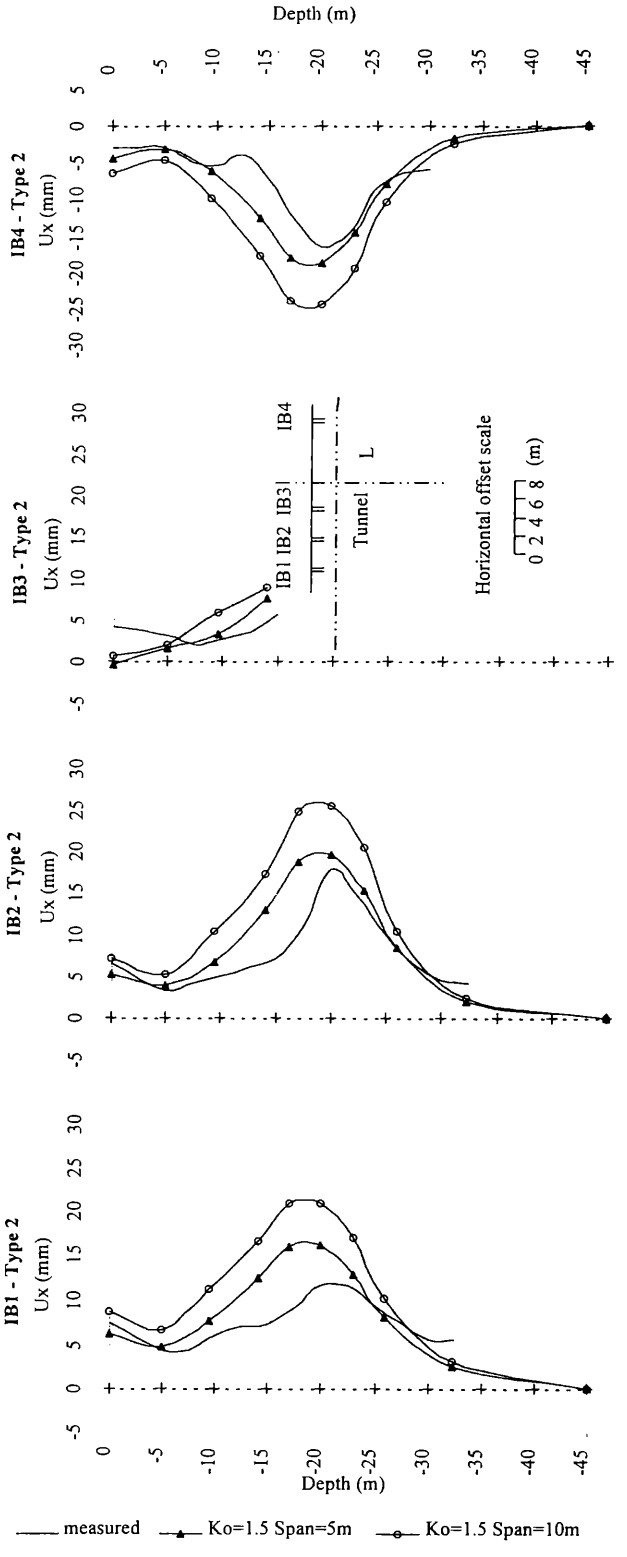


Figure 5. Lateral displacements along the depth in the middle section of the tunnel on the completion of the excavation.

It should be noted that the magnitude of the surface settlement is found to be highly dependent upon the unsupported span length during excavation. This result is consistent with the findings observed

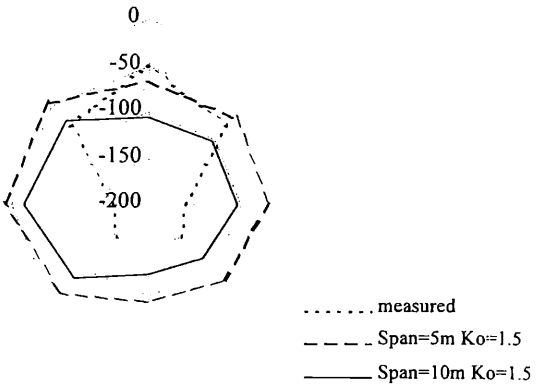


Figure 6. Excess pore pressure at the transverse section.

by Kuhnhennn (1995) on typical collapses of NATM tunnels. He suggested that the performance of the construction depended on the quality of the workmanship as well as the length of the unsupported span ahead of the shotcrete.

### 4.2 *Lateral Displacement*

The lateral displacements along the depth in the middle section of the tunnel on the completion of the excavation are plotted in Figure 5. While the ground surface settlements are slightly underestimated, the lateral displacements are slightly overestimated in the analyses. The lateral displacements are higher on the left side than those on the right side. This is due to the nonsymmetrical excavation sequence of the tunnel. Moreover, the effect of the unsupported spans is also noticeable for the lateral displacements.

### 4.3 *Excess Pore Water Pressure*

Figure 6 shows the excess pore pressure developed at the transverse section for two different unsupported spans and compared with that measured in the site. The measured values are about symmetric with the tunnel centreline, while those from the analyses are more negative on the right side. This is due to the dissipation of the excess pore water pressure of the soil on the left during the right drift excavation. In general, the predicted excess pore pressure distribution is quite consistent with the observed values.

### 4.4 *Stress Paths*

Figures 7(a) to 7(f) show the stress paths for two different unsupported spans (i.e. span=5 m or 10 m) predicted at various locations around the tunnel opening during the excavation. The tunnel face

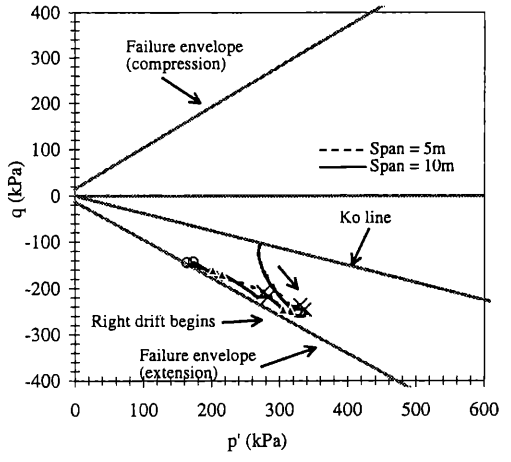


Figure 7(a). Stress path at the crown

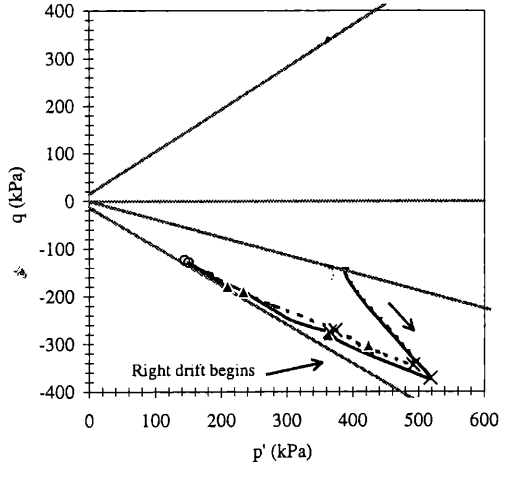


Figure 7(b). Stress path at the invert

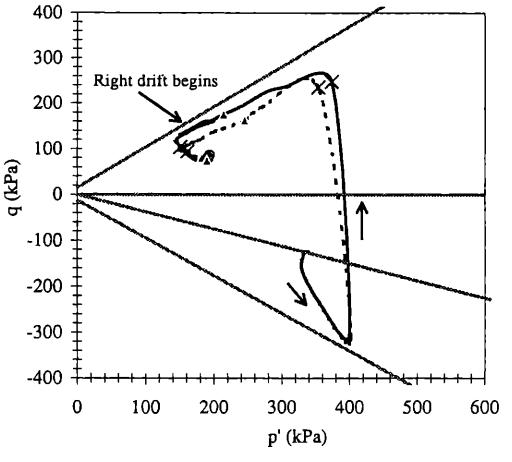


Figure 7(c). Stress path at the left springline

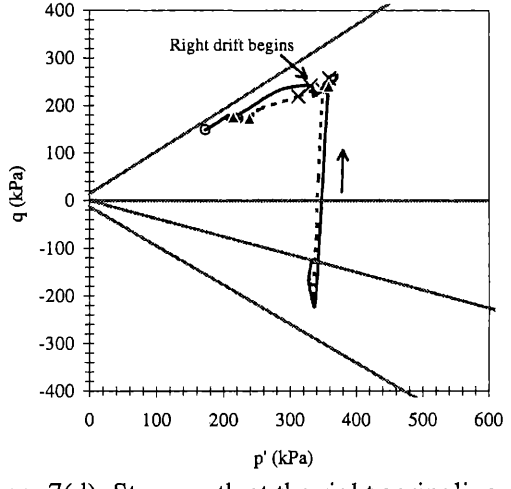


Figure 7(d). Stress path at the right springline

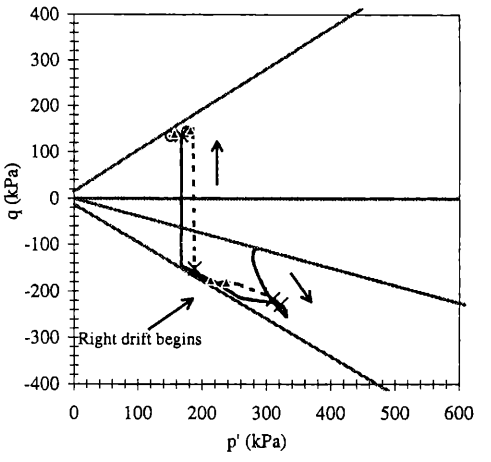


Figure 7(e). Stress path at the left shoulder

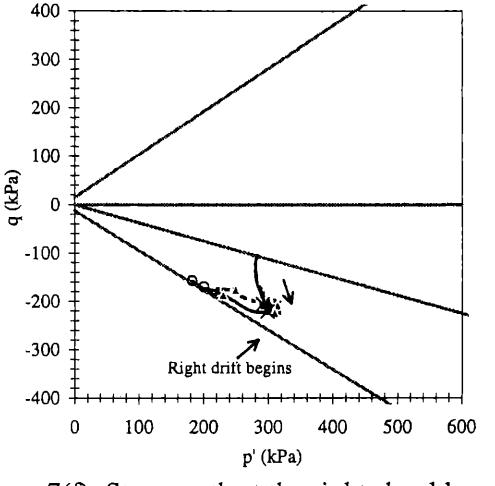


Figure 7(f). Stress path at the right shoulder

Figure 7(a)-(f). Stress path plots at various locations ($K_o$ = 1.5).

Note:
Cross means the tunnel face is at the monitoring section;
Triangle means the installation of lining is undergone at the monitoring section;
Circle means the plane strain condition at the monitoring section.

located at various distances from the monitoring section is highlighted in the figures.

One thing to notice about the convention of the deviator stress is that it is defined to be negative if the lateral effective stress is greater than the vertical effective stress.

For a larger unsupported span (i.e. span=10m), higher deviator stresses are observed to develop at the invert, at the left springline and at the left shoulder. On the other hand, a reduction in stress ratio (q/p') can be observed at the left springline. However, the effect of the unsupported span is considered to be modest.

Due to the nonsymmetrical excavation of the tunnel, the deviator stress on the left side is higher when comparing to those on the right side, at both the springlines and the shoulders. For the right springline, the stress path approaches the failure envelope, while at the left springline, the stress path moves away from the failure envelope during the right drift.

Rotation of stress is pronounced at the springlines where the stress rotation occurs in front of the tunnel face during the left drift due to arching effects. At the left shoulder, it is also observed that the stress rotation occurs but not significant at the right shoulder. The soil at the left shoulder is susceptible to compressive failure while that at the right shoulder subjected to extensive failure. This implies that the stress transfer from the right side to the left side during the right drift.

At the invert, the soil reaches failure envelope soon after the installation of the lining during the right drift and stays along the failure envelope for the rest of excavation process. This is probably because of the large tangential stress developed at the invert during the excavation. In fact, the collapse of the Heathrow Express Tunnel in London in 1994 was initiated by cracks formed. Besides the invert, the soil at the right shoulder is also subjected to extensive failure after the installation of the lining during the right drift.

## 5 CONCLUSIONS

Three-dimensional analyses were carried out to simulate the excavation of the Heathrow Express Trial Tunnel with different unsupported span lengths under the condition of Ko=1.5. Ground surface settlement, lateral displacement as well as excess pore water pressure are obtained and compared with the measured values. It has been found that the predicted values are generally consistent with those measured. Moreover, the stress paths are nonsymmetrical due to the nonsymmetrical excavation sequence. The stress paths show that the soil at the invert and at the right shoulder reaches failure during the excavation. This implies that special attention should be paid in the design and construction of tunnel invert and the right shoulder at high $K_o$ condition.

## REFERENCE


Hibbitt, Karlsson & Sorensen, Inc 1997. ABAQUS USER'S MANUAL, version 5.7.

Atzl, G.V. & J.K. Mayr 1994. FEM-analysis of Heathrow NATM Trial Tunnel. *Numerical Methods in Geotechnical Engineering, Balkema, Rotterdam:*195-201.

Burland, J.B. & J.C. Kalra 1986. Queen Elizabeth II Conference Centre: Geotechnical Aspects. *Proc. Instn. Civ. Engrs., Part 1*, 80: 1479-1503.

Chen, W. & S. Baldauf 1994. Prediction of Ground Deformation due to Excavation-Application to tunnel Lining Design in Weak Rock. *8th IACMAG*: 2565-2570. West Virginia.

Deane, A.P. & R.H. Bassett 1995. The Heathrow Express Trial Tunnel. *Proc. Instn. Civil Engineers*, 113: 144-156.

Desari, G.R., C.G. Rawlings & M.D. Bolton 1996. Numerical modelling of a NATM Tunnel Construction in London Clay. *Geotechnical Aspects of Underground Construction in Soft Ground*: 491-496. Rotterdam: Balkema.

Jenkins, J.D. & H.J. Sander 1991. Principles of the NATM and Other Uses of the Geologic Monitoring Techniques. *High Level Radioactive Waste Management*: 1105-1109. ASCE, NY, USA.

Kuhnhennn, K. 1995. Accuracy of NATM Demonstrations through Typical Failure Cases. *Proc. of Rapid Excavation and Tunnel Construction*: 667-679. USA: Sandiego.

Lee, K.M. & R.K. Rowe 1990. Finite Element Modelling of the Three-Dimensional Ground Deformation due to Tunnelling in Soft Cohesive Soils: Part 2-Results. *Computers and Geotechnics*, 10: 111-138.

Lee, K.M. & R.K. Rowe 1991. An Analysis of Three-Dimensional Ground Movements: the Thunder Bay Tunnel. *Canadian Geotechnical Journal*, 28: 25-41.

McWilliam, F. 1991. Jet Setting under Bonn. *Tunnels & Tunnelling*, April: 29-31.

Murphy, P. 1993. Design and Construction of the A20 Round Hill Tunnels. *Tunnels & Tunnelling*, April: 1993, 23-25.

New, B.M. & K.H. Bowers 1994. Ground Movement Model Validation at the Heathrow Express Trial Tunnel. *Tunnelling '94*, IMM, London: 302-329.

Peck, R.B. 1969. Deep Excavation and Tunnelling in Soft Ground. State of the Art Volume, *7th Int. Conf. on Soil Mech. & Foundation Engg*, Mexico: 225-290.

Ranken, R.E & J. Ghaboussi 1975. Tunnel Design Considerations: Analysis of Stresses and Deformations around Advancing Tunnels. *U.S. Department of Transportation, Report No. UILU-ENG75-2016.*

APPENDIX A

Table 1a. Linear Elastic Parameters of Taplow Gravel and Shotcrete.

| | Taplow Gravel | Shotcrete |
|---|---|---|
| Young's Modulus, E′ | $75x10^3$ kPa | $30x10^6$ kPa |
| Poisson's Ratio, ν | 0.2 | 0.3 |

Table 1b. Anisotropic Linear Elastic Parameters of London Clay.

| $E_v'$ | $E_h'$ | $\nu_{vh}'$ | $\nu_{hh}'$ | $G_{vh}$ |
|---|---|---|---|---|
| 7500+3900z kPa | 1.6 $E_v'$ | 0.125 | 0.125 | 0.44 $E_v'$ |

z = depth from the ground surface
*from Burland and Kalra 1986

Table 2. Drucker Prager Yield Surface and Plastic Potential Parameters.

| | Taplow Gravel | Shotcrete |
|---|---|---|
| Strength Parameters | d′ = 0.0 kPa<br>β′ = 54.8° | d′ = 14.8 kPa<br>β′ = 40.6° |
| Angle of Dilation | ν′ = 17.5° | ν′ = 11° |

Table 3. Unit Weight, Void Ratio , Coefficient of Permeability and Ko value.

| | Taplow Gravel | London Clay | Shotcrete |
|---|---|---|---|
| Dry Density | 20 kPa | 15 kPa | 24 kPa |
| Void Ratio | 0.4 | 1.0 | N/A |
| Coefficient of permeability | $1x10^{-4}$ m/s | $1x10^{-9}$ m/s | N/A |
| $K_o$ value | 0.43 | 1.5 | N/A |